APPLICATION OF NUMERICAL METHODS FOR INTEGRATING DIFFERENTIAL EQUATIONS OF CRACK EVOLUTION MODELS TO THE RANGE OF CONSTANT TENSION

Lucas Gimenis de Moura

falelucas@live.com

UTFPR

Curitiba, Paraná, Brazil

Cláudio Roberto Ávila da Silva Junior

avila@utfpr.edu.br

UTFPR

Curitiba, Paraná, Brazil

Antônio Kozlik Junior

kozlik@utfpr.edu.br

UTFPR

Curitiba, Paraná, Brazil

Waldir Mariano Machado Junior

waldir.jr@pr.senai.br

UTFPR

Curitiba, Paraná, Brazil

Abstract: *A realistic approach to structures and components used in engineering should consider the existence of cracks. The presence of cracks in structures, or mechanical components, usually, is associated with the phenomenon of fatigue, and its propagation is strongly influenced by the state of stress in its vicinity.*

In this work were obtained approximated numerical solutions through the integration of the differential equations describing the crack propagation laws of types: Paris-Erdogan, Forman, Priddle and McEvily. These laws can be formulated with the use of numerical methods of Euler, implicit and explicit, and explicit fourth-order Runge-Kutta (RK4).

Using a computational tool like the Matlab to plot graphs showing crack propagation is a didactic resource to visualize how the equations that predict crack size work and how the curves change when a parameter is altered, being useful in the study of fatigue.

The equation proposed by Paris-Erdogan sets an initial value problem (IVP), defined by a nonlinear and autonomous ordinary differential equation (ODE) of first order. More generally, the equation can be used as a Cauchy problem that consists in determining the trajectories (functions) that satisfy the differential equation, passing through the point set in the initial condition, $\left(a\left(N_0\right)=a_0\right)$. *The ODE is separable so the direct integrating method can be used to obtain solutions to the equation. Nonetheless, generally, the definition of the function "geometric correction factor" prevents the determination of the explicit function "crack size". Thus, it is possible to obtain numerical solution to the ODE, only, through the use of numerical methods.*

Keywords: *Paris-Erdogan's Law, Linear elastic fracture mechanics, IVP.*

1 MODELS OF CRACK PROPAGATION

The study of the evolution of a crack is based on the crack propagation rate. Regarding the behavior of the crack propagation rate, considering the log function of crack propagation versus the stress intensity factor on the region of an analyzed crack, the diagram can be divided into three regions indicated in Fig. 1.

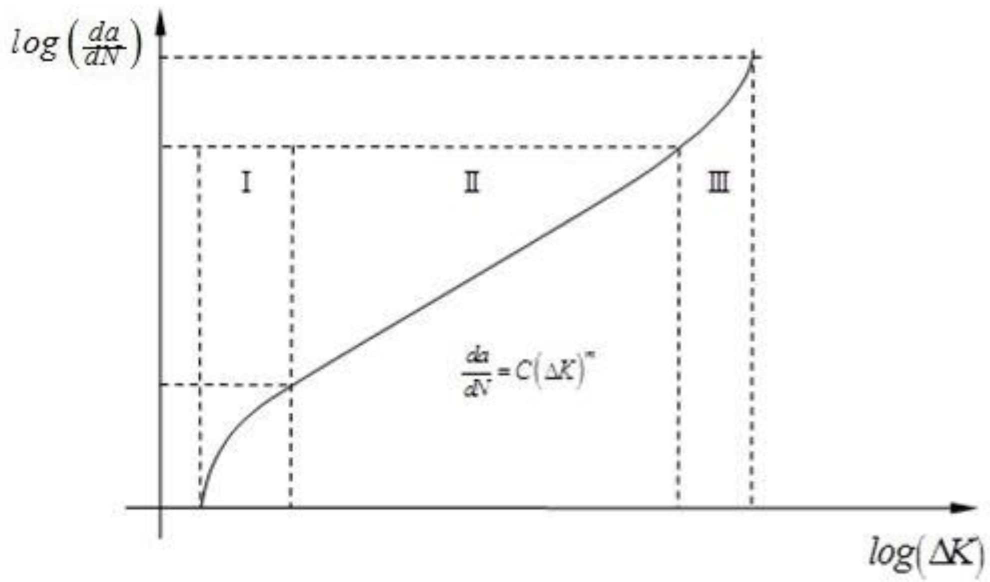

Figure 1. Diagram $log\left(\frac{da}{dN}\right)\times log\left(\Delta K\right)$**: Ávila et al. (2013).**

Region I: In this region small numerical values are observed for the stress intensity factor K and the crack behavior is associated with a limit $\left(\Delta K\right)$.

Region II: Many project methodologies based on "crack growth rate" are designed to be used in this region. Many functions have been adjusted for this region that is characterized by an approximately linear behavior. Among them stands out the equation of Paris and Erdogan (1963), that has been widely used.

Region III: This region has high crack growth rates. Generally, an instable behavior of the crack is observed in this region.

1.1 Paris-Erdogan model

The crack propagation model proposed by Paris-Erdogan describes crack growth in region II of figure 1. This model is based on experimental observations and heuristic guidelines. The evolution of a crack through this model is better represented when a probabilistic characterization is used. This is the proposed work of Ghonen & Dore (1984), which tested and analyzed results obtained from a sample of experiments for a finite plate containing a centered crack submitted to a stress load.

Using the crack propagation model proposed by Paris-Erdogan, the IVP or Cauchy problem for crack growth can be formulated according to Eq. (1).

$$\begin{cases} \text{Determine } a \in C^1([N_0, N_1]; \Re^+), \text{ such that:} \\ \dfrac{da}{dN} = C_p \Delta K^{m_p}, \forall N \in (N_0, N_1); \\ a(N_0) = a_0; \end{cases} \tag{1}$$

Cp and *mp* are parameters of the material, *N* is the number of cycles and Δ*K* is the variation of stress intensity factor.

Many variations of Paris-Erdogan model have been developed to simulate crack growth in components or structures with complex geometry, numerical analyzes have been extensively used in recent years. Among them we can mention the calculation of stress intensity factors by the boundary elements method (Leonel&Venturini, 2011; Leonel et al., 2010; Leonel et al., 2011), finite elements method (MEF) (Réthoré et al., 2010; Shen& Lew, 2010) and finite elements method Xfem (Elguedj et al., 2006; Gupta et al, 2012) including cohesive modeling of cracks.

1.2 Forman model

The Forman model (Forman et al. 1967) is used to predict the crack growth rate on fatigue in regions II and III from the diagram $log\left(\frac{da}{dN}\right) \times log\left(\Delta K\right)$ of figure 1. This model includes the effect of crack instability at the beginning of accelerated fracture and is given by Eq. (2).

$$\frac{da}{dN} = \frac{C(\Delta K)^n}{(1-R)K_c - \Delta K}, \tag{2}$$

being “n” a constant of the material. This model is in accordance with the tests performed by Broek e Shijve (1963).

1.3 Priddle model

Among the most versatile models of crack propagation is that proposed by Priddle (1976). This model describes regions I, II and III from figure 1 and is given by the Eq. (3).

$$\frac{da}{dN} = C\left(\frac{\Delta K - \Delta K_{th}}{K_c - K_{máx}}\right)^m + C', \tag{3}$$

C and *m* are parameters of the material, ΔK_{th} is the initial value where the cracks in formation starts its propagation and $K_{máx}$ the maximum stress intensity factor.

1.4 McEvily model

McEvily and Groeger (1977) proposed a model given by Eq. (4) to describe regions I, II and III from figure 1.

$$\frac{da}{dN} = \frac{A}{\sigma_y}(\Delta K - \Delta K_{th})^m \left(1 + \frac{\Delta K}{K_c - K_{máx}}\right), \tag{4}$$

being A and m parameters of the material and σ_y is the yield stress of the material. The value of ΔK_{th} is function of stress ratio R, and of the environment.

2 COMPUTATIONAL ANALYSIS

To make comparisons between numerical methods were simulated models of Paris-Erdogan, Forman, Priddle and McEvily. The integration required to obtain an evaluation of crack size is obtained from Euler, implicit and explicit, and fourth-order Runge-Kutta methods. The proposed problem is that of an infinite plate with a centered crack. It evaluated the function "crack size" for amplitude of $\Delta\sigma = 20ksi$ for a range of 900000 cycles of stress load. The software used for analyze is the MATLAB.

2.1 Paris-Erdogan model

Initially, analyzing Paris-Erdogan model for a set of data, these values were applied in Paris-Erdogan equation to evaluate crack evolution.

Parameters for solution of Paris equation, (Barsom, Rolf, 1999):

$$\begin{cases} C_p = 10^{-9}; \\ m_p = 2; \\ b = 0.5in; \\ a_0 = 0.005in; \\ N_0 = 0; \\ N_1 = 900000cycles; \\ \Delta\sigma = 20ksi, \forall N \in [0, 900000]. \end{cases}$$

Applying Euler methods, Fig. 2 shows the graphic of the curve representing the development of the crack size as a function of the number of cycles.

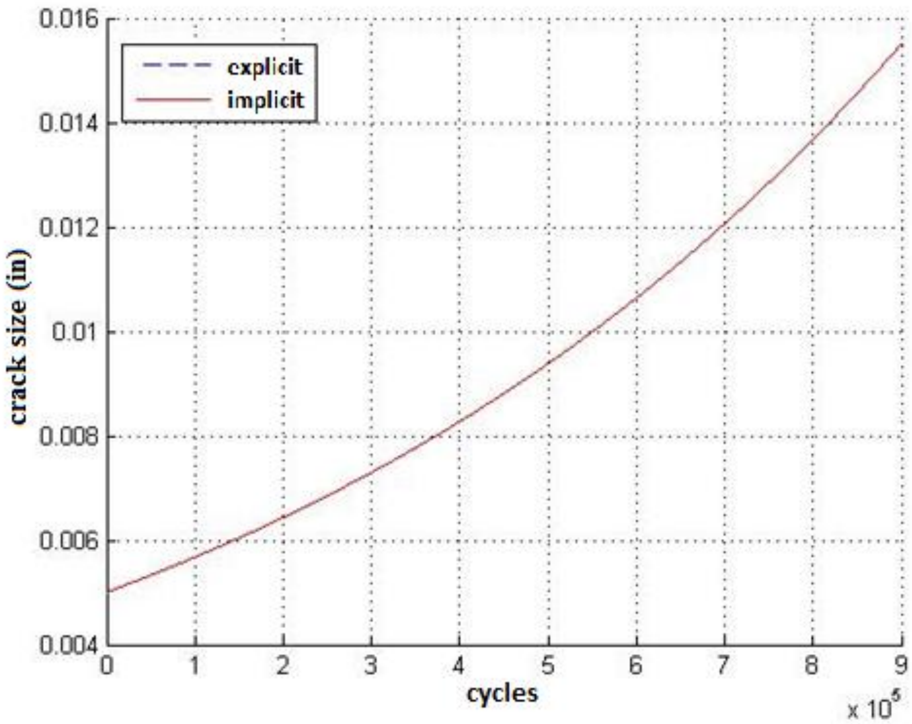

Figure 2. Evolution of the crack size using Paris model and Euler method.

Completed 900000 load application cycles, the obtained value of the crack was 15.493338*in* for the implicit method and 15.493325*in* for the explicit method. The difference between values obtained at that point was $1.318630.10^{-5}$ *in*.

Using Runge-Kutta method to 900000 cycles the crack size was 15.493336*in*. Fig. 3 shows a graphic representing the crack size, using the data provided.

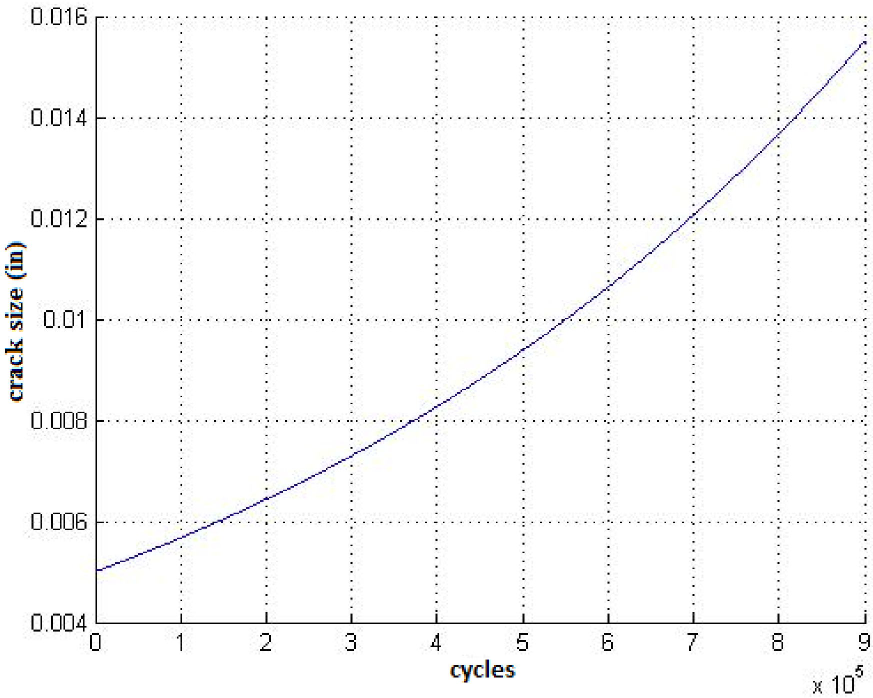

Figure 3. Evolution of the crack size using Paris model and RK4 method.

Collecting the values of different points from crack growth graphics it was possible to organize these data as observed in table 1.

Table 1 was created stipulating values for N, between 10000 cycles intervals. In this chart it is observed the following information: the values obtained for the crack size using Euler method, the difference between them, the value obtained using RK4 method and the differences between RK4 method and Euler methods, implicit and explicit.

Table 1. Values and differences between methods using Paris model.

N (number of cycles)	Implicit Euler $(a.10^{-3}\,in)$	Explicit Euler $(a.10^{-3}\,in)$	difference Implicit-Explicit $(a.10^{-3}\,in)$	Runge-Kutta-4 $(a.10^{-3}\,in)$	difference RK4-Implicit $(a.10^{-3}\,in)$	difference RK4-explicit $(a.10^{-3}\,in)$
100000	5,6694968	5,6694963	0,0000004	5,6694968	0,0000000	0,0000004
200000	6,4286476	6,4286458	0,0000018	6,4286468	-0,0000008	0,0000010
300000	7,2894488	7,2894459	0,0000029	7,2894476	-0,0000012	0,0000017
400000	8,2655119	8,2655078	0,0000041	8,2655104	-0,0000015	0,0000026
500000	9,3722705	9,3722650	0,0000055	9,3722687	-0,0000018	0,0000037
600000	10,6272248	10,6272177	0,0000071	10,6272227	-0,0000020	0,0000050
700000	12,0502184	12,0502095	0,0000089	12,0502162	-0,0000022	0,0000067
800000	13,6637518	13,6637409	0,0000109	13,6637495	-0,0000023	0,0000086
900000	15,4933384	15,4933252	0,0000132	15,4933362	-0,0000022	0,0000110

2.2 Forman model

Using Forman model, analyzes for crack growth were made for different values of loading rate R, which represents the minimum stress value divided by the maximum stress. Thus two sets of data were obtained, one for each value of R.

Parameters for solution of Forman equation, (FORMAN et al., 1967):

$$\begin{cases} C_F = 5.10^{-13}; \\ m_F = 3; \\ R = 0.1 \text{ e } 0.9; \\ K_c = 68000 lb / in^{3/2}; \\ b = 0.5 in; \\ a_0 = 0.005 in; \\ N_0 = 0; \\ N_1 = 900000 cycles; \\ \Delta\sigma = 20 ksi, \forall N \in [0, 900000]. \end{cases}$$

Initially was used the R value of 0.1 to analyze the behavior of the crack. The value obtained for the crack was 5.000000116*in* when it reaches 900000 load cycles.

It was not possible to observe measurable differences between methods for the stipulated accuracy. The modulus of the differences between the methods was null for the adopted accuracy as it is observed in table 2.

Table 2. Values and differences between methods using Forman model, R=0.1.

N (number of cycles)	Implicit Euler $(a.10^{-3}\ in)$	Explicit Euler $(a.10^{-3}\ in)$	difference Implicit-Explicit $(a.10^{-3}\ in)$	Runge-Kutta-4 $(a.10^{-3}\ in)$	difference RK4-Implicit $(a.10^{-3}\ in)$	difference RK4-explicit $(a.10^{-3}\ in)$
100000	5,00000001	5,00000001	0,00000000	5,00000001	0,00000000	0,00000000
200000	5,00000003	5,00000003	0,00000000	5,00000003	0,00000000	0,00000000
300000	5,00000004	5,00000004	0,00000000	5,00000004	0,00000000	0,00000000
400000	5,00000005	5,00000005	0,00000000	5,00000005	0,00000000	0,00000000
500000	5,00000006	5,00000006	0,00000000	5,00000006	0,00000000	0,00000000
600000	5,00000008	5,00000008	0,00000000	5,00000008	0,00000000	0,00000000
700000	5,00000009	5,00000009	0,00000000	5,00000009	0,00000000	0,00000000
800000	5,00000010	5,00000010	0,00000000	5,00000010	0,00000000	0,00000000
900000	5,00000012	5,00000012	0,00000000	5,00000012	0,00000000	0,00000000

For R value of 0.9 it was obtained a maximum crack size of 5.00000104*in* when it reaches 900000 load cycles. Again, it was not possible to observe measurable differences between methods. Table 3, shows the obtained data.

The crack size obtained for 900000 cycles was 5.0000001155*in* for R equal to 0.1 and 5.0000010429*in* for R equal to 0.9. For an R of 0.9, crack growth was 9.03 times the value obtained to a value equal to 0.1. Thus we observe, for this example, an approximately proportional and linear character between R and crack growth.

Table 3. Values and differences between methods using Forman model, R=0.9.

N (number of cycles)	Implicit Euler $(a.10^{-3}\,in)$	Explicit Euler $(a.10^{-3}\,in)$	difference Implicit-Explicit $(a.10^{-3}\,in)$	Runge-Kutta-4 $(a.10^{-3}\,in)$	difference RK4-Implicit $(a.10^{-3}\,in)$	difference RK4-explicit $(a.10^{-3}\,in)$
100000	5,00000012	5,00000012	0,00000000	5,0000001	0,00000000	0,00000000
200000	5,00000023	5,00000023	0,00000000	5,0000002	0,00000000	0,00000000
300000	5,00000035	5,00000035	0,00000000	5,0000003	0,00000000	0,00000000
400000	5,00000046	5,00000046	0,00000000	5,0000005	0,00000000	0,00000000
500000	5,00000058	5,00000058	0,00000000	5,0000006	0,00000000	0,00000000
600000	5,00000070	5,00000070	0,00000000	5,0000007	0,00000000	0,00000000
700000	5,00000081	5,00000081	0,00000000	5,0000008	0,00000000	0,00000000
800000	5,00000093	5,00000093	0,00000000	5,0000009	0,00000000	0,00000000
900000	5,00000104	5,00000104	0,00000000	5,0000010	0,00000000	0,00000000

2.3 Priddle model

For the simulations of the Priddle model it was used the data obtained in the same article where Priddle demonstrates his model for an EN3A steel.

Parameters for solution of Priddle equation, (PRIDDLE et al., 1967):
Material: EN3A Steel.

$$\begin{cases} C = 2.2.10^{-7}; \\ C' = 2.10^{-10}; \\ a_0 = 10mm; \\ N_0 = 0; \\ N_1 = 900000cycles; \\ Kc = 70MN.m^{-\frac{3}{2}}; \\ \Delta K_0 = 7MN.m^{-\frac{3}{2}}; \\ K_{máx} = 2.3MN.m^{-\frac{3}{2}}. \end{cases}$$

Analyzing table 4, when the load application reaches 900000 cycles it was obtained a crack size value of 19.744307mm for RK4 method.

Table 4. Values and differences between methods using Priddle model.

N (number of cycles)	Implicit Euler a(mm)	Explicit Euler a(mm)	difference Implicit-Explicit a(mm)	Runge-Kutta-4 a(mm)	difference RK4-Implicit a(mm)	difference RK4-explicit a(mm)
100000	10,3904495	10,3904488	0,0000007	10,3904492	-0,0000003	0,0000004
200000	10,8547231	10,8547216	0,0000015	10,8547225	-0,0000006	0,0000009
300000	11,4139521	11,4139496	0,0000026	11,4139512	-0,0000009	0,0000017
400000	12,0974011	12,0973971	0,0000040	12,0973999	-0,0000012	0,0000028
500000	12,9464326	12,9464267	0,0000059	12,9464313	-0,0000013	0,0000046
600000	14,0208447	14,0208361	0,0000085	14,0208435	-0,0000012	0,0000074
700000	15,4092528	15,4092405	0,0000123	15,4092523	-0,0000005	0,0000118
800000	17,2465708	17,2465531	0,0000176	17,2465720	0,0000012	0,0000189
900000	19,7443020	19,7442763	0,0000257	19,7443070	0,0000050	0,0000307

Using Euler methods was possible to obtain a crack growth of 9.744mm when completed 900000 cycles, as it is represented in Fig. 4.

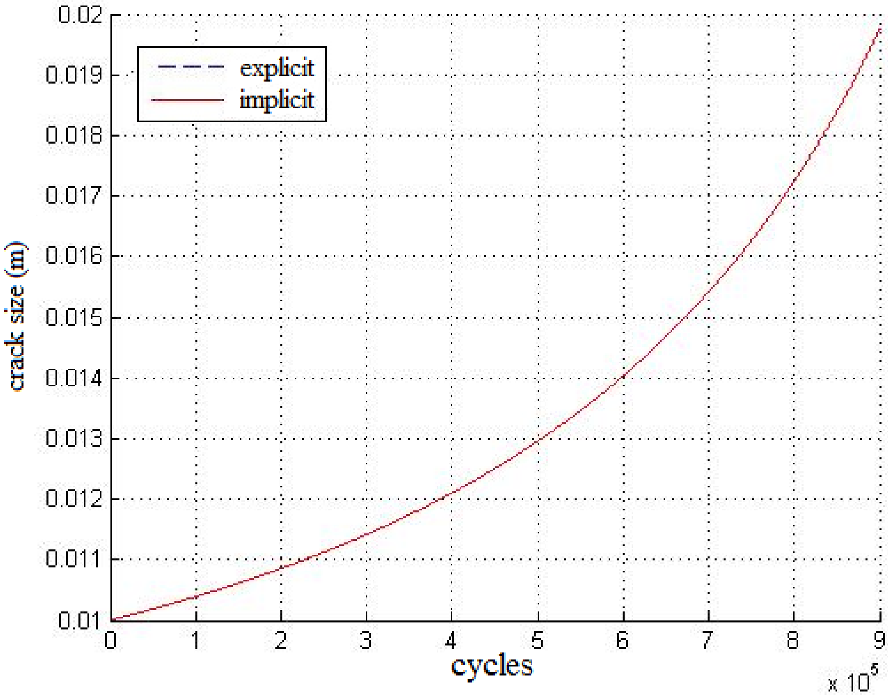

Figure 4. Evolution of the crack size using Priddle model and Euler method.

Figure 5 shows crack size values when RK4 is applied.

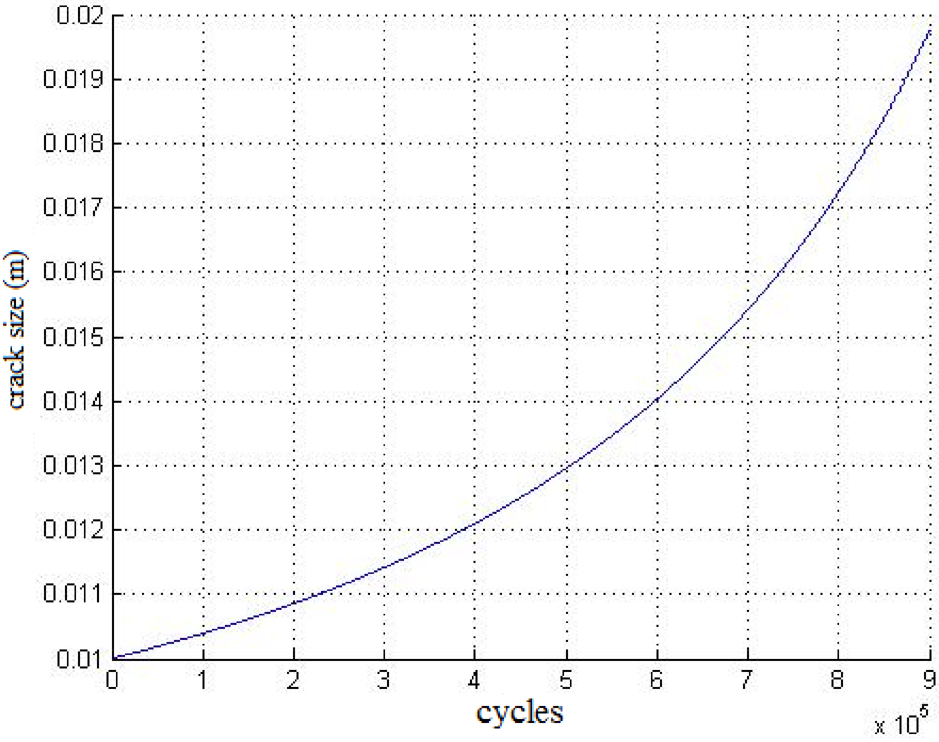

Figure 5. Evolution of the crack size using Priddle model and RK4 method.

2.4 McEvily model

For the McEvily model, the following set of data for an aluminum alloy was used to obtain crack size values.

Parameters for solution of McEvily equation, (WANG et al, 2008):
Material: 6013 aluminum alloy.

$$\begin{cases} R = 0.5; \\ \sigma_y = 448MPa \\ \Delta K_{th} = 2.20MPa\sqrt{m}; \\ K_{máx} = 2.50MPa\sqrt{m}; \\ K_c = 61.67MPa\sqrt{m}; \\ a_0 = 10mm; \\ m_m = 2; \\ \Delta\sigma = 20ksi. \end{cases}$$

For the first simulation of McEvily model, Euler method, implicit and explicit, were used to obtain the graph shown in Fig. 6, where the maximum value obtained for the crack size was 10.21779*mm* for implicit Euler .

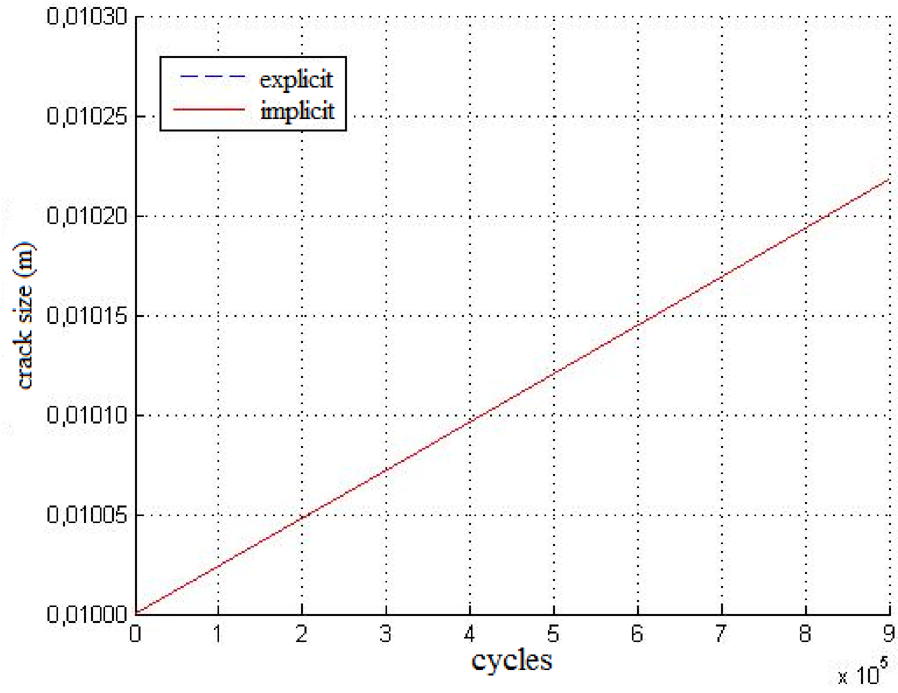

Figure 6. Evolution of the crack size using McEvily model and Euler method.

Figure 7 shows crack size values when RK4 is applied.

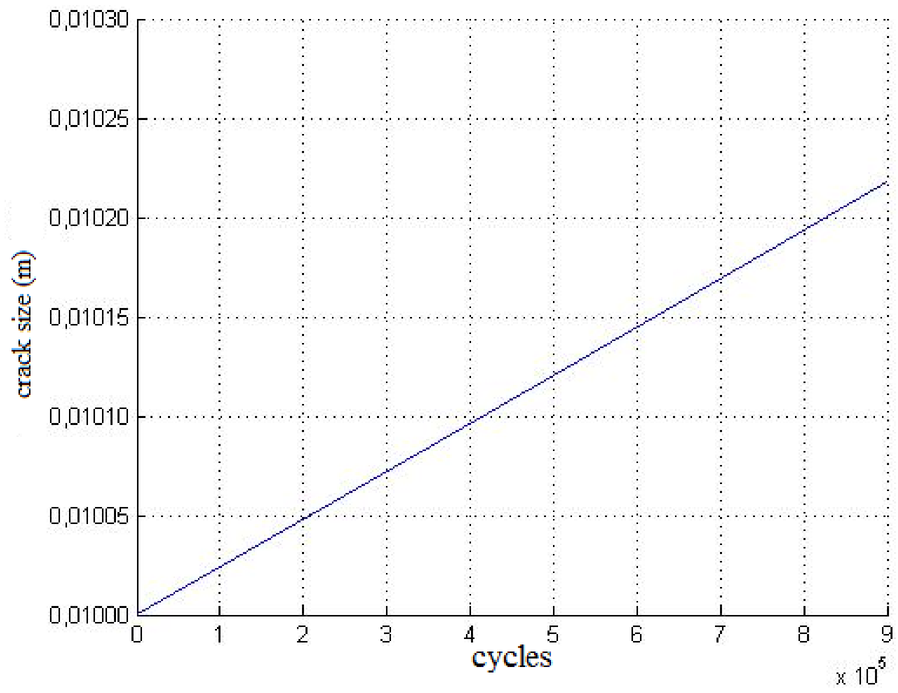

Figure 7. Evolution of the crack size using McEvily model and RK4 method.

Values for crack size were very near, as it is observed for N=900000 in table 5.

Table 5. Values and differences between methods using McEvily model

N (number of cycles)	Implicit Euler a(mm)	Explicit Euler a(mm)	difference Implicit-Explicit a(mm)	Runge-Kutta-4 a(mm)	difference RK4-Implicit a(mm)	difference RK4-explicit a(mm)
100000	10,0239123	10,0239123	0,0000000007	10,0239123	-0,0000000004	0,0000000004
200000	10,0478960	10,0478960	0,0000000014	10,0478960	-0,0000000007	0,0000000007
300000	10,0719513	10,0719513	0,0000000021	10,0719513	-0,0000000011	0,0000000011
400000	10,0960783	10,0960783	0,0000000029	10,0960783	-0,0000000014	0,0000000014
500000	10,1202773	10,1202773	0,0000000036	10,1202773	-0,0000000018	0,0000000018
600000	10,1445485	10,1445485	0,0000000043	10,1445485	-0,0000000021	0,0000000022
700000	10,1688923	10,1688923	0,0000000050	10,1688923	-0,0000000025	0,0000000025
800000	10,1933088	10,1933088	0,0000000058	10,1933088	-0,0000000028	0,0000000029
900000	10,2177984	10,2177984	0,0000000065	10,2177984	-0,0000000032	0,0000000033

3 CONCLUSIONS

As was proposed in this work, various relations between numerical methods and crack propagation models were observed. The use of numerical methods facilitates and complements initial value problems as the proposed by Paris, used as reference for other crack growth models.

The order of a method measures how quickly this method converges to the analytical solution. The inaccuracy of each method decreases when the number of steps increases. Another way to obtain more accurate values is to use methods of higher order as the Runge-Kutta.

Both, methods of Euler and RK4 method, have shown great efficacy for the integration of differential equations found in crack propagation models, and the method of highest order among the analyzed is the fourth-order Runge-Kutta. The results obtained in implicit Euler method were the nearest to those obtained using RK4 in all studied models.

Using a computational tool to plot graphs showing crack propagation is an efficient manner to visualize propagation of cracks in real engineering situations and can be used as an educational activity during the study of fatigue.

We have available several crack growth prediction models. A relevant question for engineering is the inherent cost of each type of analysis. A more complex model involving many parameters, may require additional information, usually obtained experimentally, promoting rise of costs during analyze. Moreover, depending on the required reliability of results, a simpler model may not provide the desired accuracy.

ACKNOWLEDGEMENTS

We are thankful to CILAMCE for the opportunity of participate in this congress and to Federal Technological University of Paraná for supporting our work.

REFERENCES

Ávila C, Beck AT, 2013. Efficient Bound for Crack Growth Computation.

Barsom JM, Rolfe ST, 1999. Fracture and fatigue control in structures: Applications of fracture mechanics. 3 ed. Philadelphia: ASTM.

Broek D, Schijve J, 1963. The influence of the Mean Stress on Propagation of Fatigue Cracks in Aluminum Alloy Sheet.

Elguedj T, Gravouil A, Combescure A, 2006. Appropriate extended functions for X-FEM simulation of plastic fracture mechanics, Computer Methods in Applied Mechanics and Engineering 195, 7–8, 501-515.

Forman RG, Kearney VE, Engle RM, 1967. Numerical analysis of crack propagation in cyclic loaded structures, J. Basic Engineering 89, 459-464.

Ghonem H, Dore S, 1987. Experimental study of the constant-probability crack growth curves under constant amplitude loading. Engineering Fracture Mechanics27, 1-25.

Gupta P, Pereira JP, Kim DJ, Duarte CA, Eason T, 2012. Analysis of three-dimensional fracture mechanics problems: A non-intrusive approach using a generalized finite element method, Engineering Fracture Mechanics 90, 41-64.

Leonel ED, Beck AT, Venturini WS, 2011: On the performance of response surface and direct coupling approaches in solution of random crack propagation problems, Structural Safety 33, 261-274.

Leonel ED, Chateauneuf A, Venturini WS, Bressolette P, 2010: Coupled reliability and boundary element model for probabilistic fatigue life assessment in mixed mode crack propagation. International Journal of Fatigue 32, 1823-1834.

Leonel ED, Venturini WS, 2011: Multiple random crack propagation using a boundary element formulation. Engineering Fracture Mechanics 78, 1077-1090.

McEvily AJ, Groeger J, 1977. On the threshold for fatigue crack growth. In: ICF4, Waterloo (Canada).

Paris P, Erdogan F, 1963. A critical analysis of crack propagation laws, J. Basic Eng., Trans. ASME., 85: 528-534.

Priddle EK, 1976. High cycle fatigue crack propagation under random and constant amplitude loadings. International Journal of Pressure Vessels and Piping, v. 4, n. 2, p. 89-117.

Réthoré J, Roux S, Hild F, 2010. Mixed-mode crack propagation using a Hybrid Analytical and eXtended Finite Element Method, ComptesRendusMécanique 338, 121-126.

Shen Y, Lew A, 2010. Stability and convergence proofs for a discontinuous-Galerkin-based extended finite element method for fracture mechanics, Computer Methods in Applied Mechanics and Engineering 199, 37–40, 2360-2382.

Wang Y, Cui W, Wuc X, Wang F, Huang X, 2008. The extended McEvily model for fatigue crack growth analysis of metal structures.